FtsN coordinates septal peptidoglycan synthesis and degradation through self-interaction of SPOR in *E. coli*

Zhixin Lyu[1,3], Xinxing Yang[1,4], Atsushi Yahashiri[2], Stephen Ha[1], Joshua W. McCausland[1,5], Brooke M. Britton[1], David S. Weiss[2*], Jie Xiao[1*]

[1]Department of Biophysics and Biophysical Chemistry, Johns Hopkins School of Medicine, Baltimore, MD 21205, USA.

[2]Department of Microbiology and Immunology, University of Iowa Carver College of Medicine, Iowa City, IA 52242, USA.

[3]Current address: Genetics and Biochemistry Branch, National Institute of Diabetes and Digestive and Kidney Diseases, National Institutes of Health, Bethesda, MD 20892, USA.

[4]Current address: The Chinese Academy of Sciences Key Laboratory of Innate Immunity and Chronic Disease, School of Basic Medical Sciences, Division of Life Sciences and Medicine, University of Science and Technology of China, Hefei, China.

[5]Current address: Department of Biology, Stanford University, Stanford, CA 94305 USA.

*Corresponding authors: david-weiss@uiowa.edu, xiao@jhmi.edu

Abstract

During *E. coli* cell division, the three layers of the cell envelope invaginate in a coordinated fashion. How this coordination is achieved is an open question, but the highly conserved cell division protein FtsN is a key player. FtsN activates septal peptidoglycan (sPG) synthesis through the binding of its essential (E) domain to the sPG synthase complex. It also has a C-terminal SPOR domain that binds to the PG glycan backbone at sites where stem peptides have been removed by amidases, called denuded glycans (dnGs). dnGs are subsequently degraded by lytic transglycosylases (LTs). It is proposed that dnGs in the developing division septum are a moving target that links FtsN localization and thus the activities of its associated sPG synthases in time and space to the progress of cell wall degradation. Here we examine this model using single-molecule tracking (SMT) of FtsN and the PG synthase FtsW under conditions where FtsN's interactions with dnGs or sPG synthesis activities are altered. We discovered unexpectedly that FtsN's SPOR domain self-interacts *in vivo*. These self-interactions enable FtsN to bind cooperatively *via* its SPOR domain to dnGs and to the processive synthase complex, which we propose creates a sensitive switch such that small changes of dnG availability can have a large impact on local synthesis and turnover of sPG.

Introduction

Gram-negative (diderm) bacteria such as *Escherichia coli* have a rigid cell wall composed of a thin layer of peptidoglycan (PG) formed by repeated N-acetylglucosamine (GlcNAc)-N-acetylmuramic acid (MurNAc) units cross-linked via short peptide bridges attached to MurNAc[1]. This thin PG layer is constantly remodeled by a large collection of cell wall synthases and hydrolases to allow cell growth and division. In *E. coli*, cell wall constriction during cell division requires an essential septal PG (sPG) synthase composed of the glycosyltransferase FtsW and transpeptidase FtsI along with more than ten nonessential PG hydrolases including four amidases (Ami) and eight known and putative lytic transglycosylases (LTs)[2, 3]. Amidases remove peptide crosslinks by cleaving off the peptide moiety from MurNAc, which generates denuded glycan strands (dnGs)[4, 5]. LTs cleave the β-1,4-glycosidic bond between MurNAc and GlcNAc, resulting in the removal of both dnGs and glycans with peptides[2, 6, 7]. These PG degradation processes need to be tightly controlled and coordinated with new sPG synthesis activity in time and space for robust cell wall constriction without lesions. How spatiotemporal coordination is achieved is currently unclear.

FtsN is an essential bitopic membrane protein in γ-proteobacteria. It possesses four functional domains with distinct roles in cell division: (1) a short, N-terminal cytoplasmic domain ($FtsN^{Cyto}$) that directly interacts with the early division protein FtsA to trigger the activation of FtsW[8-10]; (2) an α-helical transmembrane domain ($FtsN^{TM}$) that anchors FtsN to the inner membrane[11]; (3) a short, partially formed helical essential domain ($FtsN^{E}$) in the periplasm that binds to FtsI and its scaffolding protein FtsL to activate the sPG synthesis complex formed by FtsWI and FtsQLB[12-14]; (4) a periplasmic, C-terminal SPOR domain ($FtsN^{SPOR}$) that binds to dnG[12, 14-18]. A notable feature of FtsN is the long, largely disordered linker between $FtsN^{TM}$ and $FtsN^{SPOR}$ that also includes $FtsN^{E}$, which, when fully extended, can be ~70 nm long[14].

In our previous SMT studies in *E. coli*, we observed that FtsW, FtsI, and FtsB (and hence most likely the full sPG synthase complex formed by FtsWIQLB) exhibit two directional moving populations. One moves fast at ~30 nm s^{-1}, is inactive in sPG synthesis, and is driven by FtsZ's treadmilling dynamics through a Brownian ratchet mechanism[19-21]. We term this fast-moving

population as on the Z-track. The other population moves slowly at ~8-9 nm s^{-1}, is driven by active sPG synthesis, and is independent of FtsZ's treadmilling dynamics[19-21]. We term this slow-moving population as on the sPG synthesis track. Additionally, we observed stationary populations of FtsW, FtsI and FtsB, which we identified as either trapped to the middle of FtsZ polymers, or poised for synthesis. Thus, SMT provides a powerful means to link the moving dynamics of cell wall enzymes and regulators to their activities and functions.

We found that modulating a cell's sPG synthesis activity or FtsZ's treadmilling speed can shift the partitioning of the synthase complex between the two tracks, revealing a mechanism to coordinate sPG synthesis spatiotemporally with septal pole morphogenesis[20-22]. Such a two-track behavior was also observed in the diderm bacterium *C. crescentus*[23]. However, in Gram-positive (monoderm) bacteria such as *S. pneumoniae*[24], *B. subtilis*[25], and *S. aureus*[26], only the slow-moving, sPG synthesis-driven population of synthases was observed, likely suggesting a less stringent regulation requirement for septation and cell pole morphogenesis due to thick cell walls in these bacteria and/or a transitory Z-track-dependent behavior of these enzymes[27].

Recently, we discovered that FtsN exhibits a single, slow-moving population on the sPG-track and is a required component of the active processive synthesis complex[20, 22]. Structural modeling shows that $FtsN^{E}$ binds to FtsL and FtsI in the previously identified Activation of FtsW and FtsI (AWI) domain[28] and Constriction Control Domain (CCD)[28-30], triggering a conformational change of FtsI's Anchor domain to open up the catalytic pore of FtsW[21]. We also discovered that the moving dynamics of FtsN depend on its domain composition. For example, the isolated E domain in the absence of the rest of FtsN exhibits both the Z-track and sPG-track populations and is sufficient to maintain the processivity of the synthase complex. The cytoplasmic tail and the transmembrane domain of FtsN ($FtsN^{Cyto\text{-}TM}$) exhibits only the Z-track dependent, fast-moving population[22].

Besides the sPG-track coupled slow-moving population, we have also observed that more than half of septal FtsN molecules are stationary as they are anchored to dnGs by the SPOR domain[22]. While the essential E domain is the only region of FtsN strictly required for viability[9, 12], the SPOR domain is highly conserved and the homology is shared across a family of cell wall binding proteins in many Gram-negative and Gram-positive bacteria[12 16, 17, 31-33], suggesting its functional importance. However, the details of why so are unclear. The coexistence of a SPOR domain, which binds to dnG (a transient intermediate of sPG degradation), along with an E domain that activates the sPG synthase complex within one single protein, hints at the intriguing potential for FtsN to coordinate both sPG degradation and synthesis in time and space[18, 34]. In this work, we examine this possibility using SMT of FtsN and FtsW in different genetic backgrounds and growth conditions, aiming to understand whether there is such a coordination, and if so, how it is achieved.

Results

Altered dnG levels in Δ*amiABC* and Δ6*LT*s cells diminish sPG synthesis activity

To investigate the effect of SPOR-dnG binding on sPG synthesis activities, we monitored the moving dynamics of FtsN and FtsW using two mutant strains in which dnG levels are altered. In the Δ*amiABC* strain (strain EC5345, Supplementary Table 1), the dnG level is effectively zero due to the lack of all three amidases[12, 18], which generate dnG[7]. In the Δ6*LT*s strain (strain JL435, Supplementary Table 1), the dnG level is ~20-40 fold higher than the wildtype (WT) background[18] and cells likely have long stretches of dnG strands due to the deletion of six out of eight known and putative lytic glycosyltransferase (LTs) (Δ*mltA*, Δ*mltC*, Δ*mltD*, Δ*mltE*, Δslt*70*, Δ*rlpA*), which degrade dnG[6]. Both Δ*amiABC* and Δ6*LT*s cells showed sick chaining phenotypes due to impaired ability to degrade sPG for proper daughter cell separation[6] (Fig. 1a, b).

To perform SMT of FtsN and FtsW, we ectopically expressed a functional, previously characterized FtsN-Halo^{SW} [22] or FtsW-TagRFP-t (abbreviated as FtsW-RFP)[20] fusion protein from a plasmid in the two strain backgrounds (strains EC5345 and EC3708 respectively, Supplementary Table 1). As expected, and in accordance with altered dnG levels in the two strains, septal localization of FtsN-Halo^{SW} was reduced in Δ*amiABC* cells but enhanced in Δ6*LT*s cells (Fig. 1a, b, top; Supplementary Fig. 1a). FtsW-RFP showed similar localization levels (Fig. 1a, b, bottom; Supplementary Fig. 1b).

SMT of FtsN-Halo^{SW} and FtsW-RFP revealed that in Δ*amiABC* cells the two fusion proteins behaved similarly. The active, slow-moving populations on the sPG synthesis track for both fusions were almost completely abolished (Fig. 1c, red curves). A new fast-moving population of FtsN-Halo^{SW} appeared (P_{fm} = 41 ± 2%, n = 77 segments for FtsN-Halo^{SW}), which was similar to that of FtsW-RFP (P_{fm} = 38 ± 3%, n = 72 segments, Fig. 1c-e, blue curves and bars, Supplementary Table 4). The average lifetime of stationary FtsN-Halo^{SW} molecules decreased to T_{stat} = 9.4 ± 0.6 s (P_{stat} = 59 ± 2%, n = 109 segments, Fig. 1f, Supplementary Table 4) from T_{stat} = 27 ± 1 s we previously measured under the wild-type (WT) condition[22], comparable to that of stationary FtsW-RFP molecules (T_{stat} = 9.1 ± 0.6 s, n = 116 segments, Fig. 1f, Supplementary Table 4). This shortened stationary lifetime is similar to the average lifetime of stationary FtsZ molecules (8-12 s) measured in *E. coli* and other species[22, 24, 35-37]. As there is essentially no dnG in Δ*amiABC* cells, these results suggest that stationary FtsN-Halo^{SW} and FtsW-RFP molecules are the ones captured in the middle of treadmilling FtsZ polymers as we and others previously observed both *in vivo* and *in vitro*[20, 22, 38].

In Δ6*LT*s, FtsN-Halo^{SW} and FtsW-RFP also behaved similarly to each other. The majority of the fusion protein molecules were stationary (P_{stat} = 91 ± 3%, n = 546 segments for FtsN-Halo^{SW} and P_{stat} = 88 ± 3%, n = 252 segments for FtsW-RFP, respectively, Fig. 1d, e, black curves and gray bars, Supplementary Table 4), consistent with the expectation that an elevated dnG level increases dnG-bound FtsN-Halo^{SW} molecules and consequently FtsN-bound FtsW-RFP molecules. Most strikingly, the stationary lifetime of FtsN-Halo^{SW}, which reflects the time it takes for single FtsN-Halo^{SW} molecules to dissociate from dnG, increased to T_{stat} = 59 ± 2 s in Δ6*LT*s cells (Fig. 1f, Supplementary Table 4). The marked increase in both the percentage and dissociation time of stationary FtsN-Halo^{SW} molecules in Δ6*LT*s cells, coupled with the elevated dnG level, suggests enhanced FtsN binding affinities. As an elevated dnG level corresponds to a greater number of SPOR domain binding sites, the rise in binding affinity with increased number

of binding sites and bound FtsN molecules supports a cooperative binding mechanism. Similar phenomena have been observed on the length-dependent binding of oligomeric DNA- or mRNA-binding proteins[39-41]. The stationary lifetime of FtsW-RFP molecules also increased to T_{stat} = 24 ± 1 s (Fig. 1f, Supplementary Table 4), up from ~18 s in WT conditions we measured previously[20], suggesting FtsW's binding to dnG-anchored FtsN may be mediated by a similar cooperative mechanism under this condition.

The lack of a slow-moving population of FtsN-Halo^{SW} and FtsW-RFP in the two strains indicates the lack of active sPG synthesis[20, 22]. To verify this result, we used HADA (HCC-Amino-D-alanine hydrochloride) labeling to measure the septal cell wall synthesis activity as we previously described[42]. As shown in Fig. 1g, h, both strains showed significantly lower HADA incorporation levels than that of WT cells, which were also indistinguishable from that of sPG synthesis-inhibited cells treated with cephalexin. The lack of septal cell wall synthesis activity in Δ*amiABC* cells is consistent with minimal septum localization of FtsN in the absence of dnG (Fig.1a). In Δ6*LT*s cells, however, as both FtsN-Halo^{SW} and FtsW-RFP showed predominantly stationary populations due to the elevated dnG level, these results strongly suggest that dnG-binding sequesters FtsN (and consequently FtsN-bound FtsW), which needs to be released from dnG to activate sPG synthesis.

Truncation of FtsN's SPOR domain leads to the sequestering of FtsW on the Z-track

To examine the role of the FtsN-dnG interaction without modulating dnG levels, we constructed a FtsN$^{\Delta SPOR}$ strain in which the *spor* sequence is deleted from the full-length *ftsN* gene at its native chromosomal locus (strain EC3338, Supplementary Table 1). Cells expressing the *ftsN*$^{\Delta SPOR}$ truncation gene grew slowly and were filamentous, but restored to WT-like growth and similar septum synthesis activity when an additional copy of *ftsN*$^{\Delta SPOR}$ is expressed from a plasmid (strain JL337, termed as *ftsN*$^{\Delta SPOR+}$ herein below for simplicity, Supplementary Table 1, Supplementary Fig. 2). These results are consistent with the expectation that SPOR is the major septum localization determinant of FtsN and hence a higher expression level of FtsN$^{\Delta SPOR}$ is needed to support cell division at a similar level.

Next, we performed single-molecule tracking of FtsW-RFP expressed from a plasmid in the *ftsN*$^{\Delta SPOR+}$ background (strain JL362, Supplementary Table 1) using the same M9 minimal medium and imaging conditions as before[22]. We observed that the sPG synthesis processivity of FtsW, which we define as the average persistent run time of the active, slow-moving population (T_{sm}), remained similar in the absence of SPOR (T_{sm} = 21.1 ± 0.5 s, μ ± s.e.m. in *ftsN*$^{\Delta SPOR+}$ *vs.* 20.1 ± 0.1 s in WT, Fig. 2c, top, Supplementary Fig. 3, Supplementary Table 5). The persistent run time of FtsW on the Z-track remained unchanged as well (T_{fm} = 9.4 ± 0.2 s, μ ± s.e.m. in *ftsN*$^{\Delta SPOR}$ *v.s.* 8.3 ± 0.3 s in WT, Fig. 2c, bottom, Supplementary Table 5). However, the active, slow-moving population of FtsW-RFP decreased significantly (from 33 ± 2%, n = 157 segments in WT strain to 8 ± 3%, n = 38 segments in *ftsN*$^{\Delta SPOR+}$ strain), while the fast-moving population increased from 12 ± 2% to 19 ± 2% (Fig. 2a, b, Supplementary Table 5). Additionally, the stationary population of FtsW-RFP increased to 73.5 ± 2% (n = 353 segments, Fig. 2a, b, Supplementary Table 5) from ~55% under WT conditions as we previously reported[20] and had a short lifetime at T_{stat} = 10.4 ± 0.4 s (Supplementary Table 5). This stationary lifetime is comparable to that of FtsW-RFP in Δ*amiABC* (Supplementary Table 4), suggesting that they were similarly stuck in the middle of FtsZ polymers. Taken together, these results suggest that in the absence

of FtsN's SPOR domain, while FtsW's processivities on the sPG- and Z-tracks are largely unaltered, FtsW is primarily sequestered on the Z-track, with a reduced slow-moving population on the sPG-track.

Truncation of FtsN's SPOR domain leads to the sequestering of FtsN$^{\Delta SPOR}$ on the Z-track and reduces its sPG-track processivity

To examine how the deletion of the SPOR domain affects the moving dynamics of FtsN itself, we constructed a chromosomal integrated FtsN$^{\Delta SPOR}$-Halo^{SW} fusion protein and overexpressed it in an *ftsN*-depletion background (strain EC5257, Supplementary Table 1) to restore normal cell length. We observed that the stationary population of FtsN$^{\Delta SPOR}$-Halo^{SW} at septa decreased to 40% ± 2% with an average T_{stat} = 9.2 ± 0.6 s (n = 85 segments, Fig. 2c, d, Supplementary Table 5), suggesting that they were trapped in the middle of FtsZ polymers as well. Most importantly, in contrast to the singular slow-moving population observed for FtsN-Halo^{SW}, FtsN$^{\Delta SPOR}$-Halo^{SW} exhibited two distinct processively-moving populations, one slow (P_{sm} = 13 ± 3%, V_{sm} = 9.4 ± 0.1 nm s^{-1}, μ ± s.e.m., n = 28 segments) and one fast (P_{fm} = 46 ± 2%, V_{fm} = 32.7 ± 0.1 nm s^{-1}, μ ± s.e.m., n = 98 segments, Fig. 2b, d, Supplementary Table 5). Inhibiting sPG synthesis activity using aztreonam completely abolished the slow-moving population of FtsN$^{\Delta SPOR}$-Halo^{SW} but preserved the fast-moving population (Fig. 2b, e, Supplementary Table 5), similar to what we previously observed for FtsW in aztreonam-treated cells[20] or FtsB in fosfomycin-treated cells[21]. However, the run times of FtsN$^{\Delta SPOR}$-Halo^{SW} on both the sPG-track and the Z-track (T_{sm} = 7.5 ± 0.1 s and T_{fm} = 5.5 ± 0.1 s respectively, Fig. 2c, Supplementary Table 5) were shorter than those of FtsW-RFP in the *ftsN*$^{\Delta SPOR}$ background (Supplementary Table 5) and the full-length FtsN-Halo^{SW} on the sPG-track (14.5 ± 0.7 s, Fig. 2c). These results suggest that similar to FtsW in the absence of FtsN's SPOR domain, FtsN$^{\Delta SPOR}$-Halo^{SW} was mainly sequestered on the FtsZ-track. Because dnG-bound FtsN molecules are stationary and not running on the sPG synthesis track[22], the reduced run time of FtsN$^{\Delta SPOR}$-Halo^{SW} on the sPG-track suggests that the SPOR domain may have a role in supporting the processivity of FtsN in the active sPG synthesis complex independent of its dnG-binding ability.

An FtsN^{Q251E} mutant defective in dnG-binding partially restores FtsN's sPG synthesis track population

Truncation of FtsN's SPOR domain removes both the dnG-binding ability and potentially other, non dnG-binding-dependent, interactions of the SPOR domain. To further investigate the effects of these two types of interactions, we monitored the moving dynamics of a FtsN^{Q251E}-Halo^{SW} fusion protein by transforming a *ftsN*^{Q251E}-*halo*^{SW} expressing plasmid into an FtsN-depletion strain (strain JL378, Supplementary Table 1). FtsN^{Q251E} diminishes the binding of FtsN to dnG significantly due to the critical mutation Q251E in the SPOR domain's dnG binding cleft but maintains its folding stability and hence potential protein-protein interactions[43].

Consistent with a defect in dnG-binding, FtsN^{Q251E}-Halo^{SW} exhibited a smaller, 42 ± 2% stationary population with a significantly reduced stationary lifetime at T_{stat} = 13.1 ± 0.9 s (n = 81 segments) and a fast-moving population on the Z-track (P_{fm} = 33 ± 2%, T_{fm} = 6.4 ± 0.2 s, n = 64 segments, Fig. 2b, c, f, Supplementary Table 5). These results further confirm that the dnG-binding ability of SPOR prevents the release of FtsN to the Z-track. Interestingly, the slow-moving population percentage and processivity of FtsN^{Q251E}-Halo^{SW} recovered to P_{sm} = 25 ± 2% and T_{sm} = 9.7 ± 0.2 s (n = 49 segments), in between that of FtsN$^{\Delta SPOR}$-Halo^{SW} and full-length FtsN-Halo^{SW} (Fig. 2b, c, f, Supplementary Table 5). These results suggest that there likely exist non dnG-

binding-dependent interactions of the SPOR domain that can partially restore FtsN's sPG-track population and its processivity on the sPG-track.

Isolated SPOR domain (iSPOR) moves processively with WT FtsN

To further investigate the role of SPOR in supporting FtsN's slow-moving population on the sPG-track independent of other FtsN domains, we made use of a previously characterized fusion construct FtsN^{WYAA}-Halo^{SW}. This fusion protein contains two critical mutations W83A and Y85A in FtsN's E domain (FtsN^{E}), which abolish the binding of FtsN^{E} to FtsI and FtsL and the subsequent activation of FtsWI[9, 44]. We previously reported that FtsN^{WYAA}-Halo^{SW} molecules were completely stationary at septa in the superfission variant *ftsB*^{E56A} Δ*ftsN* background, despite that FtsW-RFP still moved processively on the sPG-track in the same strain background.

Surprisingly, when we ectopically expressed this FtsN^{WYAA}-Halo^{SW} fusion protein in the presence of WT FtsN (Fig. 3a, strain EC5259, Supplementary Table 1), we observed that it exhibited essentially the same percentage of the slow-moving population compared to WT FtsN-Halo^{SW} (P_{sm} = 44 ± 4%, n = 79 segments, Fig. 3b, c, Supplementary Table 6) with a modestly reduced processivity (T_{sm} = 10.7 ± 0.8 s, Fig. 3d, top, Supplementary Table 6). This result suggests that FtsN^{WYAA}-Halo^{SW} remains part of the processively-moving sPG synthase complex through its binding to WT FtsN in the complex, as its direct binding of the E domain with FtsI and FtsL is abolished by the WYAA mutations, and that it stops moving in the absence of WT FtsN in the superfission *ftsB*^{E56A} Δ*ftsN* background[22].

Our previous studies showed that the cytoplasmic and transmembrane domains of FtsN are not involved in the formation of the processive sPG complex[22]. Therefore, we reasoned that the SPOR domain must be responsible for such interaction in the absence of the E domain-mediated binding to FtsI and FtsL. We constructed a Halo-iSPOR fusion protein in which a Halo-tag is fused to the N-terminus of the isolated SPOR domain (hereafter termed iSPOR to distinguish from the SPOR domain linked to the rest of FtsN) and expressed it in the presence of WT FtsN (Fig. 3e, strain EC5275, Supplementary Table 1). Strikingly, while Halo-iSPOR localized to the septum as expected (Supplementary Fig. 4), these Halo-iSPOR molecules also exhibited a similar percentage for the slow-moving population (P_{sm} = 42 ± 3%, n = 61 segments, Fig. 3c, f, Supplementary Table 6) with a processivity of T_{sm} = 9.8 ± 0.7 s (Fig. 3d, top, Supplementary Table 6). In cells treated with aztreonam, Halo-iSPOR became predominately stationary (Supplementary Fig. 5) mimicking what we observed on full-length FtsN-Halo^{SW} previously[22]. These results strongly suggest that there may exist SPOR-SPOR self-interaction.

iSPOR^{Q251E} defective in dnG binding moves processively with WT FtsN

One alternative explanation for the observed processive movement of iSPOR with WT FtsN is that iSPOR and FtsN's SPOR domain may bind to the same dnG fragments disintegrated from the cell wall without direct protein-protein interactions. To examine this possibility, we constructed an isolated Halo-iSPOR^{Q251E} fusion, which is defective in dnG-binding, and expressed it in the WT FtsN background (Fig. 3g, strain JL431, Supplementary Table 1). Surprisingly, Halo-iSPOR^{Q251E} still exhibited a large slow-moving population with a similar processivity (P_{sm} = 36 ± 4%, T_{sm} = 9.6 ± 0.6 s, n = 33 segments, Fig. 3c, d, h, Supplementary Table 6). This experiment demonstrates that the observed iSPOR-FtsN interaction is independent of dnG-binding. Note that the moving dynamics of Halo-iSPOR^{Q251E} in the presence of WT FtsN mimics that of WT FtsN but not that of FtsN^{Q251E}-Halo^{SW}. The latter exhibited a fast-moving population (compare Fig. 2f and

Fig. 3h). This comparison further confirms that there must exist SPOR-SPOR self-interaction in the processive sPG synthase complex.

iSPOR becomes stationary when disconnected from the rest of FtsN

To further verify that iSPOR binds to the existing SPOR domain of full-length FtsN in the processive sPG synthesis complex, we expressed Halo-iSPOR *in trans* with FtsN$^{\Delta SPOR+}$ (Fig. 3i, strain EC5415, which also contains an extra plasmid copy of *ftsN*$^{\Delta SPOR}$, Supplementary Table 1). Halo-iSPOR localized to the septum in the FtsN$^{\Delta SPOR+}$ background similarly as that in the WT FtsN background (Supplementary Fig. 4). We reason if the movement of iSPOR is due to its binding to FtsN domains other than SPOR, we should still observe its processive movement with FtsN$^{\Delta SPOR+}$. However, Halo-iSPOR molecules became completely stationary (Fig. 3c, j) with a stationary lifetime at T_{stat} = 29.2 ± 1.3 s (n = 602 segments, Supplementary Table 6) that is indistinguishable with that of full-length FtsN-Halo^{SW} (Fig. 1f). Treating cells with aztreonam did not change the percentage nor the lifetime of these stationary Halo-iSPOR molecules (Fig. 3c, d, Supplementary Fig. 5). Note that the stationary lifetimes of the FtsN^{WYAA}-Halo^{SW}, Halo-iSPOR and Halo-iSPOR^{Q251E} in the presence of WT FtsN were shorter and in the range of~15-20 s (Fig. 3d, bottom, Supplementary Table 6), suggesting that these iSPOR domains may not compete with WT FtsN for dnG binding. Consistent with this suggestion, we observed that when cells were treated with aztreonam, full-length FtsN-Halo^{SW} was stuck at the septum, while both Halo-iSPOR and FtsN$^{\Delta SPOR}$-Halo^{SW} left the septum in time-lapse movies (Supplementary Fig. 6, Supplementary Movies 1-3).

Most importantly, as we showed in Fig. 2, in the same *ftsN*$^{\Delta SPOR+}$ strain background, FtsW-RFP and FtsN$^{\Delta SPOR}$-Halo^{SW} exhibited both slow- and fast-moving populations. Therefore, these results strongly suggest that SPOR-SPOR self-interaction and the linkage between SPOR and the rest of FtsN are responsible for the observed processive movement of iSPOR. As such, these results demonstrate that the active, processive FtsWIQLB-FtsN complex contains multiple FtsN molecules mediated by SPOR-SPOR self-interaction, and that this interaction is important to maintain the percentage of active sPG synthase complex on the sPG synthesis track.

Stationary and processive sPG synthase complexes are non-monomeric

In our single-molecule tracking experiments, we used sparse Halo-dye (JF646) labeling to ensure the tracking of single molecules of interest. We also screened out fluorescence spots with intensities higher than single molecules. In light of the above results, we reexamined some of our data to assess whether we could directly visualize the presence of more than one molecule in the same stationary and processive sPG synthesis complexes. Indeed, we identified FtsN-Halo^{SW} molecules in both moving and stationary SMT trajectories where the fluorescent spot intensities are significantly higher than expected from a single JF646 dye molecule and exhibited the typical quantized photobleaching step or fluorescence jump for single molecules (Fig. 3k). We even observed one FtsN-Halo^{SW} molecule repeatedly associated and dissociated until it finally joined a processively moving complex stably (Fig. 3k, left). Most importantly, we identified similar trajectories showing the presence of more than one single molecule from our previous SMT of Halo-FtsB[21], FtsI-Halo^{SW} [19] and FtsW-RFP[20] fusions in *E. coli* and Halo-FtsW in *C. crescentus*[23] (Supplementary Fig. 7). Thus, while the sparse labeling prevents us from further statistical analysis of the number of molecules in the complex, these observations demonstrate that the FtsWIQLB-FtsN complex in *E. coli* exists as a multimer in the form of (FtsWIQLB)$_m$-FtsN$_n$ or (FtsWIQLB-FtsN)$_n$. The non-monomeric nature of the sPG synthase complex may be a conserved

feature across different bacterial species, as a recent SMT study in *B. subtilis* also observed the presence of multimeric PBP2b, the equivalent of FtsI in *E. coli*, on the sPG synthesis track[25].

Relative sPG synthesis and degradation activities are correlated in WT FtsN background but skewed when SPOR is disconnected

Under balanced growth and division conditions, sPG synthesis and degradation activities need be correlated to avoid aberrant cell pole morphogenesis or septal cell wall lesions. In other words, high synthesis activity should correspond to high degradation activity and low synthesis activity should correspond to low degradation activity in order to have concurrent inward growth of new sPG and cleavage of old sPG. FtsN has been proposed to be a key player in coordinating these two opposing activities due to its E domain's binding to the sPG synthase complex and SPOR domain's binding to dnG, a transient PG degradation intermediate[18, 34].

Our observation that FtsN exhibits two populations, one slow-moving in complex with active FtsWIQLB and the other stationary in complex with dnG, naturally leads to a correlation between sPG synthesis and degradation activities: binding of FtsN to processive FtsWIQLB activates sPG synthesis while exposing dnGs to degradation by LTs, and *vice versa*. Indeed, we found that overexpressing iSPOR in WT cells caused a profound chaining phenotype (Supplementary Fig. 8), suggesting iSPOR protects dnG from being degraded by LTs, consistent with a previous study[45].

To evaluate the correlation quantitatively, we compared FtsN's distributions on dnG and the processive sPG synthesis track (Fig. 4). We first calculated the product of the slow-moving population percentage of FtsN and the corresponding processive run length under each condition, normalized to that of the WT condition, and used it as the proxy for sPG synthesis activity (see "Methods" section). Using FtsW-RFP or FtsI-Halo^{SW} data instead of FtsN-Halo^{SW} as the proxy for sPG synthesis activity produced similar results (Supplementary Fig. 9). We then calculated the product of the percentage of the stationary population of FtsN-Halo^{SW} and its corresponding stationary lifetime, normalized to that of the WT condition, as a proxy for the dnG level in cells. The inverse of the dnG level should reflect sPG degradation activity (high dnG levels indicate low LT activities and low dnG levels indicate high LT activities).

Indeed, Fig. 4a showed that relative sPG synthesis is correlated to the inverse of the dnG level across a variety of conditions. For example, in cells harboring a superfission variant FtsI^{R167S} and grown in rich medium, sPG synthesis activity is high while the dnG level is low. In cells treated with cell wall synthesis inhibitors (MTSES for *ftsW*^{I302C}, aztreonam or fosfomycin) or deleted of six LTs, sPG synthesis activity was low and dnG level was high. The relative synthesis and dnG level of a modified FtsN variant that lacks the cytoplasmic and transmembrane domains (Halo-FtsN$^{\Delta Cyto-TM}$) also largely followed the same trend (Fig. 4a), indicating that the correlation is unrelated to the cytoplasmic interactions of FtsN with FtsA.

Most importantly, we found that on average, the ratio of the inverse of dnG level, or the pseudo sPG degradation activity, to the sPG synthesis activity was close to one across all conditions but became significantly higher at ~6 when cells expressing Halo-iSPOR in *trans* with *ftsN*$^{\Delta SPOR}$ were treated with aztreonan to inhibit sPG synthesis (Fig. 4b). These results hence suggest that the linking of the SPOR domain to the rest of FtsN is required to maintain balanced sPG synthesis and degradation activities.

Discussion

Taken together and built on our previous two-track model, we propose an updated model of how septal cell wall synthesis and degradation are coordinated. In addition to the previously proposed sPG synthesis track, represented by the slow-moving, active FtsWIQLB-FtsN complex, and the Z-track, represented by treadmilling FtsZ polymers and the fast-moving, inactive FtsWIQLB complex[20], we now introduce a third, the sPG degradation track, represented by the stationary population of FtsN (Fig. 4c). Because FtsN protects dnG from being degraded by LTs and simultaneously sequesters FtsWIQLB, the release of FtsWIQLB-FtsN from dnG allows for concurrent initiation of new sPG synthesis and dnG degradation at the same time and in the same place. As such, the dynamic re-distribution of FtsWIQLB between the Z- and sPG synthesis tracks facilitates the even distribution of enzymes and consequently smooth, symmetric septum growth as we previously proposed, while FtsWIQLB's distribution between the sPG synthesis and degradation tracks places new sPG synthesis activity close to sPG degradation sites.

Self-interaction of SPOR

The following evidence supports the presence of self-interaction of FtsN's SPOR domain both when bound to dnG and when bound to active FtsWIQLB. First, FtsN is expressed at a level about 3-4-fold higher than FtsW, I, and QLB[22, 46], making it possible to form at least $(\text{FtsWIQLB-FtsN})_n$ type of complexes. Second, in our previous Structured Illumination Microscopy imaging experiments, we observed large FtsN clusters either remaining stationary or moving processively together[22]. Third, in our current single-molecule tracking experiments, we directly observed the presence of more than one FtsN molecule in the stationary or slow-moving trajectories (Fig. 3k). Fourth, $\text{FtsN}^{\text{WYAA}}$ moved processively in the presence of full-length WT FtsN (Fig. 3a), but became completely stationary when *ftsN* is deleted in the superfission $ftsB^{E56A}$ background[22]. Similarly, iSPOR moved processively in the presence of full-length WT FtsN (Fig. 3e, f), but not in the presence of $\text{FtsN}^{\Delta\text{SPOR+}}$ (Fig. 3i, j). Finally, $\text{iSPOR}^{\text{Q251E}}$, which is defective in dnG binding, still exhibited similar percentages of the slow-moving population and the stationary population (Fig. 3g, h, Supplementary Table 4). These observations strongly support the presence of SPOR-SPOR self-interaction independent of dnG binding on both the degradation and synthesis tracks.

We have tried to characterize the self-interaction of iSPOR *in vitro* but were largely unsuccessful. Purified iSPOR showed a single monomeric species in size exclusion columns and static light scattering (Supplementary Fig. 11, Supplementary Table 7). Crosslinking experiments to trap transient interactions revealed oligomers at high iSPOR concentrations, but it cannot be excluded that the crosslinked oligomers arise from random collisions (Supplementary Fig. 12). The published NMR structure of iSPOR shows a monomer[14]. Thus, *in vitro* support for the SPOR-SPOR interaction we observe *in vivo* is lacking. One possible explanation is that the interaction requires one of the partners be full-length FtsN. The Loose group has indeed shown that full-length FtsN *in vitro* forms a dimer in sedimentation experiments[38].

Cooperative binding of SPOR to dnG

Several findings argue FtsN's SPOR domain binds cooperatively to dnG. First, we observed that not only the stationary population percentages, but also the stationary lifetime of single FtsN molecules, changed in response to a variety of altered conditions (Figs.1-3). As the lifetime of a single molecule at a particular state reflects the time it takes to exit that state, the stationary lifetime of single FtsN molecules is the direct measurement of its apparent dnG-dissociation time constant. These changes are therefore consistent with altered binding affinities

between dnG and SPOR, in addition to shifted binding equilibria where only the bound and unbound population percentages change.

Second, while we could not directly quantify dnG level or length under different conditions, FtsN's binding affinity responded to expected dnG levels in cells. For example, FtsN's stationary lifetime increased ~2-fold to ~60 s in the Δ6*LT*s mutant, where the dnG level is ~20-40 fold higher than that of WT cells (Fig. 1f)[18]. iSPOR in a $FtsN^{\Delta SPOR+}$ background had a similar stationary lifetime as that of full-length FtsN (~30 s, Fig. 3d, bottom), but in the presence of WT FtsN, iSPOR's stationary lifetime decreased to ~20 s and further to ~14 s when cells were treated with aztreonam (Fig. 3d, bottom). In contrast, full-length FtsN's stationary lifetime increased to ~40 s in cells treated with aztreonam[22]. These results strongly suggest that the decreased binding affinity of iSPOR to dnG in the presence of WT FtsN is due to a low dnG level, as most dnG was occupied by full-length FtsN. The few-fold change in the binding affinities of SPOR to dnG, together with *in vivo* evidence for a SPOR-SPOR self-interaction, is most consistent with a cooperative binding mechanism, which has been frequently observed in DNA/mRNA-length-dependent cooperative binding of oligomeric proteins[39-41]. Notably, previously the Vollmer group demonstrated that purified FtsN periplasmic domain binds exclusively to dnG strands >25 NAM-NAG units, consistent with a cooperative binding mechanism[17].

Third, we considered an alternative that changes in the stationary lifetime of FtsN are not due to the cooperative binding of SPOR to dnG, but active "pulling" of SPOR from dnG by processive sPG synthases or "pushing" away from dnG by processive LTs. We reason active "pulling" by processive sPG synthases is unlikely because iSPOR (with $FtsN^{\Delta SPOR+}$), which does not have an E domain to bind to the sPG synthase complex, had the same stationary lifetime as that of full-length WT FtsN (Fig. 3d, bottom). Active "pushing" of SPOR away from dnG by processive LTs is also unlikely because overexpression of iSPOR led to a strong chaining phenotype (Supplementary Fig. 8), suggesting that LTs are unable to "push" iSPOR off dnG.

Finally, all stationary lifetime distributions of FtsN under these conditions exhibited non-exponential distributions (Supplementary Fig. 10), indicating that the underlying process cannot be described as a single rate-limiting step. Many of these distributions contained a rise and decay, a signature for multiple, consecutive steps[47], which would be consistent with a cooperative, non-monomeric process. By this logic, the affinity of $FtsN^{SPOR}$ depends on the length of a dnG strand, and the long-tails in the stationary lifetime plots (Supplementary Fig. 10) arise from long dnGs.

It is unclear whether the self-interaction of SPOR on the sPG synthesis track is also cooperative, but the processive run time distributions of FtsN showed similarly a rise and decay as that of FtsN's stationary lifetime distribution (Supplementary Figs. 3, 10). Notably, FtsW's slow-moving populations also showed non exponential distributions (Supplementary Fig. 3). It is likely that these self-interactions are also cooperative, but further experiments are required to examine this possibility.

Biological function of cooperativity of SPOR

What would be the biological function of cooperative self-interaction of SPOR domains? Cooperativity is often observed in biology when a switch-like behavior in response to a small change in protein or substrate concentration is required. For example, when LTs activities are low (as mimicked here using the Δ6*LT*s mutant), tight binding of FtsN to dnG can sequester nearly all sPG synthase complexes on the sPG degradation track to lower the corresponding sPG synthesis activity. When sPG synthesis activity is low (as mimicked here with aztreonam or Fosfomycin

treatment), diminished slow-moving population of FtsN renders not only more FtsN molecules anchored to dnG but also tighter binding (stationary lifetime at ~40 s), hence impeding LTs' activities on dnG (Fig. 4a, left part). Conversely, when sPG synthesis activities are high (such as in the superfission mutant *ftsI*^{R167S}, the rich medium EZRDM, or increased lipid II conditions), more FtsN molecules are bound to the processively-moving sPG synthase complex, making fewer FtsN molecules available to bind dnG with lower affinities (stationary lifetime at ~14 s). Therefore, more dnG is exposed to LTs for degradation (Fig. 4a, right part).

Furthermore, cooperativity can strengthen the binding reaction of SPOR on either the sPG degradation or the sPG synthesis track, facilitating their respective functions. For example, truncation of SPOR led to a significant reduction in the slow-moving population of FtsW and the processivity of FtsN on the synthesis track, suggesting that SPOR's self-interaction on the synthesis track likely enhances the binding of FtsN to the synthase complex, and hence increasing the activated population percentage of the complex.

We note that the truncation of SPOR did not impact the processivity of FtsW. The persistent run time of FtsW on the sPG-track was ~20 s regardless of the presence or absence of FtsN's SPOR domain (Supplementary Table 5). In contrast, the persistent run time of FtsN$^{\Delta SPOR}$ was only ~7 s, and that of full-length FtsN was ~14 s, both significantly shorter than those of FtsW and FtsI under the same conditions (Supplementary Table 5). This apparent discrepancy raises an interesting possibility, that is, there is a cycling of multiple FtsN molecules in the processive sPG syntheses complex. While each FtsN molecule only binds the processive sPG synthase complex for ~14 s on average, there is always at least one FtsN molecule in the complex to maintain FtsWI's processivity for ~20 s. One example trajectory in Fig. 3k may indeed suggest this process.

Lastly, the cooperative binding of SPOR to dnG likely makes the capturing of FtsWIQLB-FtsN dissociated from the sPG synthesis track more efficient, which helps prevent release to the Z-track. However, SPOR-dnG binding affinity needs to be in the right range. When the binding is too tight as in the Δ6*LT*s background, all FtsWIQLB-FtsN are sequestered on dnG and sPG synthesis activity is diminished. When there is no SPOR-dnG binding as that in the Δ*amiABC* background, all complexes are sequestered on the Z-track and sPG synthesis activity is also diminished. We also note that as Δ6*LT*s and Δ*amiABC* may have other significant defects other than just different dnG levels, further experiments are required to investigate these effects.

FtsN ensures balanced sPG synthesis and degradation activities

Our results show that under most conditions where an intact FtsN copy is present, the normalized sPG synthesis and degradation activities are proportional to each other, i.e., balanced. However, in cells where the SPOR domain (iSPOR) is severed from the rest of the FtsN, this balance was broken (Fig. 4a, b, red). A previous study using FDAA (fluorescent D-amino acid) to measure septal cell wall synthesis and degradation in *E. coli* showed that an *ftsN*$^{\Delta SPOR}$ background led to a higher sPG degradation/synthesis rate ratio than that in WT cells[48], consistent with our observation that a SPOR domain connected to the rest of FtsN is required to maintain the proper balance between the two activities. Note that under this condition the synthesis rate decreased but the degradation rate did not, suggesting that possibly other SPOR protein may help protect dnG in the absence of FtsN's SPOR domain. Interestingly, this work also showed that a superfission *ftsL** (*ftsL*^{E88K}) background led to a lower degradation/synthesis rate ratio. This strain still contained a functional full-length FtsN. It would be interesting to examine whether FtsN

binding to this mutant FtsL is altered, as the mutation E88K is next to E87 that is involved in the binding with FtsN's E domain[21].

FtsN coordinates sPG synthesis and degradation both in space and time

Finally, our results are consistent with a model in which FtsN not only coordinates sPG synthesis and degradation at the activity level, but also in time and space (Fig. 4c). SPOR-dnG binding may provide a spatial and timely cue to FtsWI complexes so that new sPG synthesis occurs in the vicinity of old, denuded sPG strands and at the time when the dnG is newly generated by amidases and before it is degraded by LTs.

Specifically, FtsN binds to dnG generated by amidases, protecting them from being degraded by LTs. The sPG synthase complex FtsWIQLB remains in complex with stationary, dnG-bound FtsN through the binding of FtsI and FtsL to FtsN's E domain. When FtsN's SPOR domain dissociates from dnG and sPG precursors are available, the FtsWIQLB-FtsN complex initiates processive sPG synthesis, allowing new synthesis to occur in the vicinity of dnG. Simultaneously, the dissociation of FtsN's SPOR domain from dnG allows LTs to degrade dnG, thus destroying the old binding sites for FtsN. Similarly, when FtsWIQLB-FtsN moves processively to synthesize new sPG, the long, flexible linker of FtsN between the SPOR and E domains may allow SPOR to probe for the presence of newly generated dnGs. Once found, SPOR binds to the newly generated dnG, potentially bringing the entire FtsWIQLB-FtsN complex to commence another round of sPG synthesis nearby. This iterative cycling of sPG synthesis and degradation coordinates the two activities spatiotemporally.

References

1. Vollmer, W. & Bertsche, U. Murein (peptidoglycan) structure, architecture and biosynthesis in *Escherichia coli*. *Biochim. Biophys. Acta* **1778**, 1714-1734 (2008).
2. van Heijenoort, J. Peptidoglycan hydrolases of *Escherichia coli*. *Microbiol. Mol. Biol. Rev.* **75**, 636-663 (2011).
3. Jorgenson, M.A., Chen, Y., Yahashiri, A., Popham, D.L. & Weiss, D.S. The bacterial septal ring protein RlpA is a lytic transglycosylase that contributes to rod shape and daughter cell separation in *Pseudomonas aeruginosa*. *Mol. Microbiol.* **93**, 113-128 (2014).
4. Heidrich, C. *et al.* Involvement of N-acetylmuramyl-L-alanine amidases in cell separation and antibiotic-induced autolysis of *Escherichia coli*. *Mol. Microbiol.* **41**, 167-178 (2001).
5. Priyadarshini, R., de Pedro, M.A. & Young, K.D. Role of peptidoglycan amidases in the development and morphology of the division septum in *Escherichia coli*. *J. Bacteriol.* **189**, 5334-5347 (2007).
6. Scheurwater, E., Reid, C.W. & Clarke, A.J. Lytic transglycosylases: bacterial space-making autolysins. *Int. J. Biochem. Cell Biol.* **40**, 586-591 (2008).
7. Vollmer, W., Joris, B., Charlier, P. & Foster, S. Bacterial peptidoglycan (murein) hydrolases. *FEMS Microbiol. Rev.* **32**, 259-286 (2008).
8. Busiek, K.K. & Margolin, W. A role for FtsA in SPOR-independent localization of the essential Escherichia coli cell division protein FtsN. *Mol. Microbiol.* **92**, 1212-1226 (2014).
9. Liu, B., Persons, L., Lee, L. & de Boer, P.A. Roles for both FtsA and the FtsBLQ subcomplex in FtsN-stimulated cell constriction in *Escherichia coli*. *Mol. Microbiol.* **95**, 945-970 (2015).
10. Pichoff, S., Du, S. & Lutkenhaus, J. The bypass of ZipA by overexpression of FtsN requires a previously unknown conserved FtsN motif essential for FtsA-FtsN interaction supporting a model in which FtsA monomers recruit late cell division proteins to the Z ring. *Mol. Microbiol.* **95**, 971-987 (2015).
11. Dai, K., Xu, Y. & Lutkenhaus, J. Topological characterization of the essential *Escherichia coli* cell division protein FtsN. *J. Bacteriol.* **178**, 1328-1334 (1996).
12. Gerding, M.A. *et al.* Self-enhanced accumulation of FtsN at Division Sites and Roles for Other Proteins with a SPOR domain (DamX, DedD, and RlpA) in *Escherichia coli* cell constriction. *J. Bacteriol.* **191**, 7383-7401 (2009).
13. Park, K.T., Johnson, D.K., Pichoff, S., Du, S. & Lutkenhaus, J. The essential domain of FtsN triggers cell division by promoting interaction between FtsL and FtsI. *bioRxiv* (2023).
14. Yang, J.C., Van Den Ent, F., Neuhaus, D., Brevier, J. & Lowe, J. Solution structure and domain architecture of the divisome protein FtsN. *Mol. Microbiol.* **52**, 651-660 (2004).
15. Alcorlo, M. *et al.* Structural basis of denuded glycan recognition by SPOR domains in bacterial cell division. *Nat. Commun.***10**, 5567 (2019).
16. Moll, A. & Thanbichler, M. FtsN-like proteins are conserved components of the cell division machinery in proteobacteria. *Mol. Microbiol.* **72**, 1037-1053 (2009).
17. Ursinus, A. *et al.* Murein (peptidoglycan) binding property of the essential cell division protein FtsN from *Escherichia coli*. *J. Bacteriol.* **186**, 6728-6737 (2004).
18. Yahashiri, A., Jorgenson, M.A. & Weiss, D.S. Bacterial SPOR domains are recruited to septal peptidoglycan by binding to glycan strands that lack stem peptides. *Proc. Natl Acad. Sci. USA* **112**, 11347-11352 (2015).
19. McCausland, J.W. *et al.* Treadmilling FtsZ polymers drive the directional movement of sPG-synthesis enzymes via a Brownian ratchet mechanism. *Nat. Commun.* **12**, 609 (2021).
20. Yang, X. *et al.* A two-track model for the spatiotemporal coordination of bacterial septal cell wall synthesis revealed by single-molecule imaging of FtsW. *Nat. Microbiol.* **6**, 584-593 (2021).

21. Britton, B.M. *et al.* Conformational changes in the essential E. coli septal cell wall synthesis complex suggest an activation mechanism. *Nat. Commun.* **14**, 4585 (2023).
22. Lyu, Z. *et al.* FtsN maintains active septal cell wall synthesis by forming a processive complex with the septum-specific peptidoglycan synthases in *E. coli*. *Nat. Commun.* **13**, 5751 (2022).
23. Mahone, C.R. *et al.* Integration of cell wall synthesis and chromosome segregation during cell division in *Caulobacter*. *J. Cell Biol.* **223** (2024).
24. Perez, A.J. *et al.* Movement dynamics of divisome proteins and PBP2x:FtsW in cells of *Streptococcus pneumoniae*. *Proc. Natl Acad. Sci. USA* **116**, 3211-3220 (2019).
25. Whitley, K.D. *et al.* Peptidoglycan synthesis drives a single population of septal cell wall synthases during division in *Bacillus subtilis*. *Nat. Microbiol.* (2024).
26. Schaper, S. *et al.* Cell constriction requires processive septal peptidoglycan synthase movement independent of FtsZ treadmilling in *Staphylococcus aureus*. *Nat. Microbiol.* (2024).
27. Perez, A.J. & Xiao, J. Stay on track - revelations of bacterial cell wall synthesis enzymes and things that go by single-molecule imaging. *Curr. Opin. Microbiol.* **In press** (2024).
28. Park, K.T., Du, S. & Lutkenhaus, J. Essential role for FtsL in activation of septal peptidoglycan synthesis. *mBio* **11**, e03012 (2020).
29. Condon, S.G.F. *et al.* The FtsLB subcomplex of the bacterial divisome is a tetramer with an uninterrupted FtsL helix linking the transmembrane and periplasmic regions. *J. Biol. Chem.* **293**, 1623-1641 (2018).
30. Marmont, L.S. & Bernhardt, T.G. A conserved subcomplex within the bacterial cytokinetic ring activates cell wall synthesis by the FtsW-FtsI synthase. *Proc. Natl Acad. Sci. USA* **117**, 23879-23885 (2020).
31. Smith, T.J. & Foster, S.J. Characterization of the involvement of two compensatory autolysins in mother cell lysis during sporulation of *Bacillus subtilis*. *J. Bacteriol.* **177**, 3855-3862 (1995).
32. Mishima, M. *et al.* Solution structure of the peptidoglycan binding domain of *Bacillus subtilis* cell wall lytic enzyme CwlC: characterization of the sporulation-related repeats by NMR. *Biochemistry* **44**, 10153-10163 (2005).
33. Arends, S.J. *et al.* Discovery and characterization of three new *Escherichia coli* septal ring proteins that contain a SPOR domain: DamX, DedD, and RlpA. *J. Bacteriol.* **192**, 242-255 (2010).
34. Yahashiri, A., Jorgenson, M.A. & Weiss, D.S. The SPOR domain, a widely conserved peptidoglycan binding domain that targets proteins to the site of cell division. *J. Bacteriol.* **199** (2017).
35. Squyres, G.R. *et al.* Single-molecule imaging reveals that Z-ring condensation is essential for cell division in *Bacillus subtilis*. *Nat. Microbiol.* **6**, 553-562 (2021).
36. Buss, J. *et al.* A multi-layered protein network stabilizes the *Escherichia coli* FtsZ-ring and modulates constriction dynamics. *PLoS Genet.* **11**, e1005128 (2015).
37. Barrows, J.M., Anderson, A.S., Talavera-Figueroa, B.K. & Goley, E.D. Intrinsic and extrinsic factors regulate FtsZ function in *Caulobacter crescentus*. *bioRxiv* (2023).
38. Baranova, N. *et al.* Diffusion and capture permits dynamic coupling between treadmilling FtsZ filaments and cell division proteins. *Nat. Microbiol.* **5**, 407-417 (2020).
39. Peisley, A. *et al.* Kinetic mechanism for viral dsRNA length discrimination by MDA5 filaments. *Proc. Natl Acad. Sci. USA* **109**, E3340-3349 (2012).
40. Morrone, S.R. *et al.* Cooperative assembly of IFI16 filaments on dsDNA provides insights into host defense strategy. *Proc. Natl Acad. Sci. USA* **111**, E62-71 (2014).
41. Hooy, R.M. & Sohn, J. The allosteric activation of cGAS underpins its dynamic signaling landscape. *eLife* **7** (2018).

42. Yang, X. *et al.* GTPase activity-coupled treadmilling of the bacterial tubulin FtsZ organizes septal cell wall synthesis. *Science* **355**, 744-747 (2017).
43. Duncan, T.R., Yahashiri, A., Arends, S.J., Popham, D.L. & Weiss, D.S. Identification of SPOR domain amino acids important for septal localization, peptidoglycan binding, and a disulfide bond in the cell division protein FtsN. *J. Bacteriol.* **195**, 5308-5315 (2013).
44. Du, S., Pichoff, S. & Lutkenhaus, J. FtsEX acts on FtsA to regulate divisome assembly and activity. *Proc. Natl Acad. Sci. USA* **113**, 5052-5061 (2016).
45. Yakhnina, A.A. & Bernhardt, T.G. The Tol-Pal system is required for peptidoglycan-cleaving enzymes to complete bacterial cell division. *Proc. Natl Acad. Sci. USA* **117**, 6777-6783 (2020).
46. Li, G.W., Burkhardt, D., Gross, C. & Weissman, J.S. Quantifying absolute protein synthesis rates reveals principles underlying allocation of cellular resources. *Cell* **157**, 624-635 (2014).
47. Floyd, D.L., Harrison, S.C. & van Oijen, A.M. Analysis of kinetic intermediates in single-particle dwell-time distributions. *Biophys. J.* **99**, 360-366 (2010).
48. Navarro, P.P. *et al.* Cell wall synthesis and remodelling dynamics determine division site architecture and cell shape in *Escherichia coli*. *Nat. Microbiol.* **7**, 1621-1634 (2022).

Figures and Legends

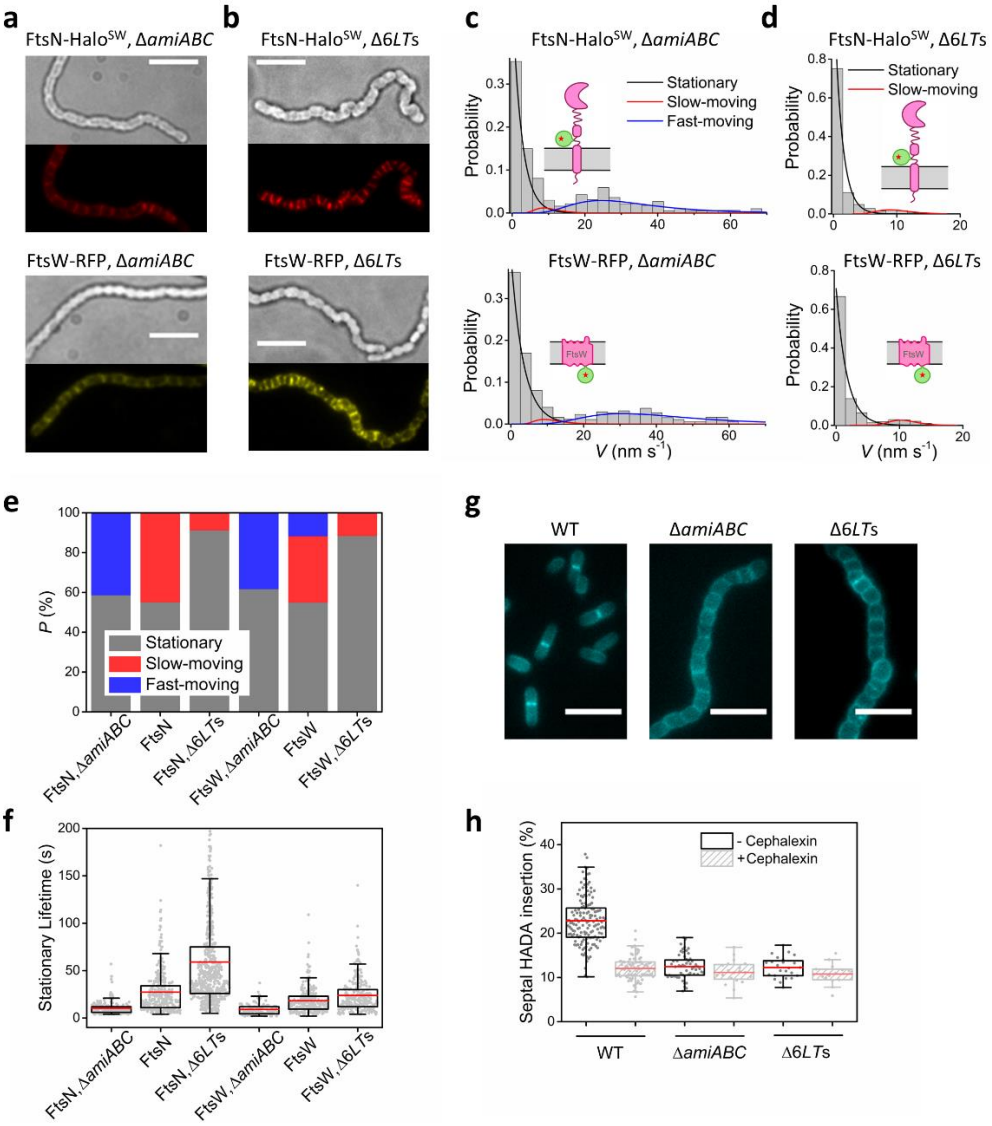

Fig.1 Altered dnG level modulates sPG synthesis activity.

a-b, Bright-field and ensemble fluorescent images of FtsN-Halo^{SW} (top) and FtsW-RFP (bottom) fusions in Δ*amiABC* (**a**) and Δ6*LT*s (**b**) strain backgrounds. Scale bars, 5 µm. **c-d**, Speed distributions of FtsN-Halo^{SW} (top) and FtsW-RFP (bottom) in Δ*amiABC* (**c**) and Δ6*LT*s (**d**) strain backgrounds overlaid with the fit curves of the stationary (black), slow-moving (red), and fast-moving (blue) populations. Schematic representation of the fusion and strain backgrounds are shown in inset (pink: labeled protein; green: Halo or RFP fluorophore). **e**, Percentage of the stationary (gray), slow-moving (red), and fast-moving (blue) populations of FtsN-Halo^{SW} and FtsW-RFP fusions in WT, Δ*amiABC*, and Δ6*LT*s strain backgrounds. **f**, Box plots of the lifetime of the stationary population under all the conditions in **e**. Red lines indicate the mean values. **g**, Representative images of HADA-labeled WT, Δ*amiABC*, and Δ6*LT*s cells. Scale bars, 5 µm. **h**, Box plots of septal HADA fluorescence intensity percentage normalized to the whole cell intensity in WT, Δ*amiABC*, and Δ6*LT*s cells.

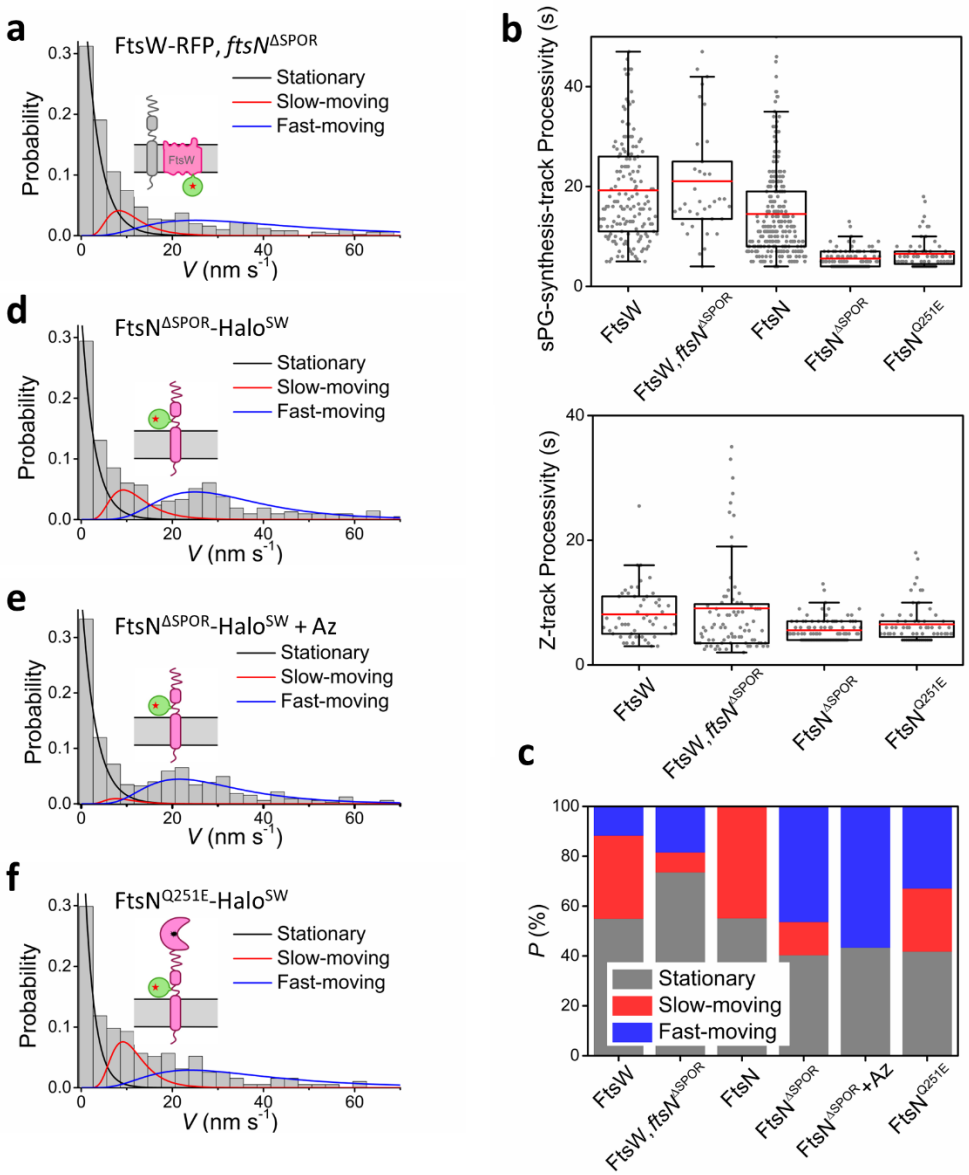

Fig.2 SPOR domain enhances FtsW and FtsN's slow-moving population.

a, **d-f**: Speed distributions of FtsW-RFP in an *ftsN*$^{\Delta SPOR+}$ background (**a**), FtsN$^{\Delta SPOR}$-Halo^{SW} in *ftsN*$^{\Delta SPOR+}$ strain background (**d**) and treated with aztreonam (**e**), and FtsN^{Q251E}-Halo^{SW} (**f**) overlaid with the fit curves of the stationary (black), slow-moving (red), and fast-moving (blue) populations. Schematic representation of the fusion and strain background are shown in insets. **b**, Percentage of the stationary (gray), slow-moving (red), and fast-moving (blue) populations under all the conditions in **a**, **d**, **e**, **f**. FtsW and FtsN data were replotted from figure **1e** for comparison. **c**, sPG synthesis track processivity (top; defined as the lifetime of the slow-moving population) and Z-track processivity (bottom; defined as the lifetime of the fast-moving population) under the conditions in **b**.

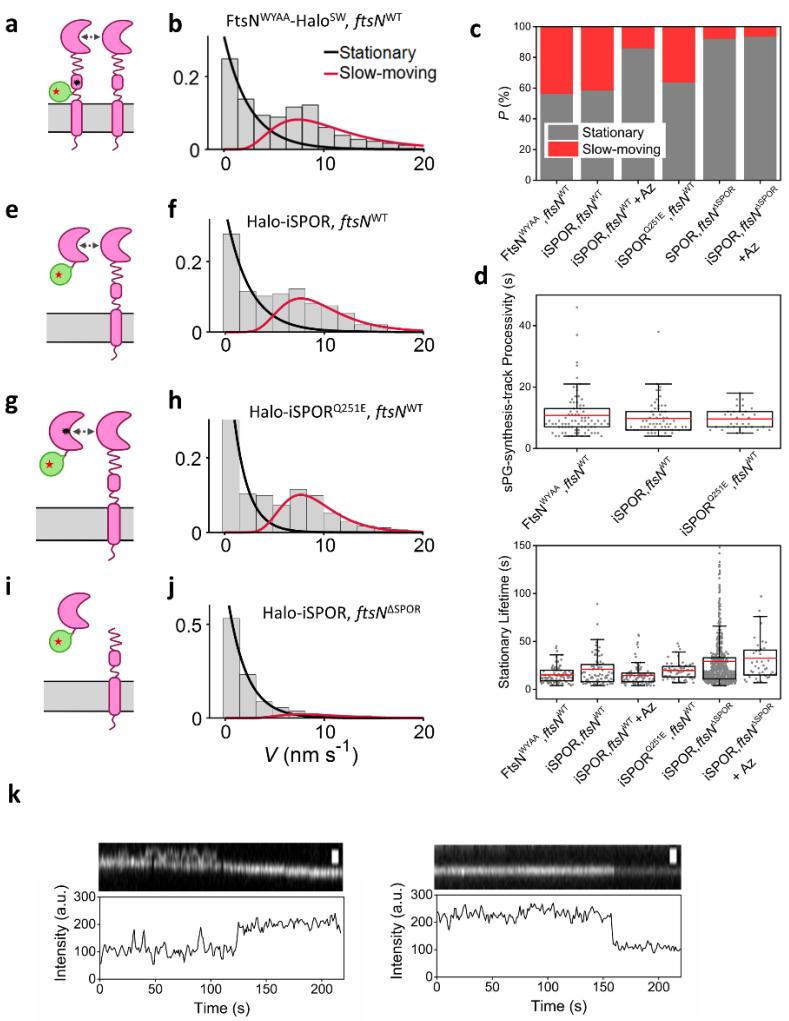

Fig.3 SPOR domain exhibits SPOR-SPOR self-interaction.

a-**b**, Schematic representation of FtsN^{WYAA}-Halo^{SW} fusion in WT FtsN background (**a**) and the speed distribution of FtsN^{WYAA}-Halo^{SW} overlaid with the fit curves of the stationary (black) and slow-moving (red) populations (**b**). **c**, Percentages of the stationary (gray) and slow-moving (red) populations under all the conditions in **b**, **f**, **h**, **j**, and **S3**. **d**, Top: sPG synthesis track processivity of FtsN^{WYAA}-Halo^{SW}, Halo-iSPOR, and Halo-iSPOR^{Q251E} fusions in WT strain. Bottom: Stationary lifetime of all the conditions in **c**. **e**-**f**, Schematic representation of Halo-iSPOR fusion in WT FtsN background (**e**) and the speed distribution of Halo-iSPOR overlaid with corresponding fit curves (**f**). **g**-**h**, Schematic representation of Halo-iSPOR^{Q251E} fusion in WT FtsN background (**g**) and the speed distribution of Halo-iSPOR^{Q251E} overlaid with corresponding fit curves (**h**). **i**-**j**, Schematic representation of Halo-iSPOR fusion in *ftsN*$^{\Delta SPOR+}$ strain background (**i**) and the speed distribution of Halo-iSPOR overlaid with corresponding fit curves (**j**). **k**, Representative kymographs (top) and intensity time traces (bottom) of FtsN-Halo^{SW} multimers at the septum. Left: an FtsN-Halo^{SW} molecule transitorily associated and disassociated (diffusive fluorescence intensity) with a processively moving FtsN-Halo^{SW} molecule (stable fluorescence intensity) between 20 s and 100 s, and eventually stably associated (sudden doubling of fluorescence intensity) and moved together at an average speed of 7 nm s^{-1}; Right: one FtsN-Halo^{SW} molecule was photo-bleached (~155 s) in a stationary dimer. Scale bars, 1 µm.

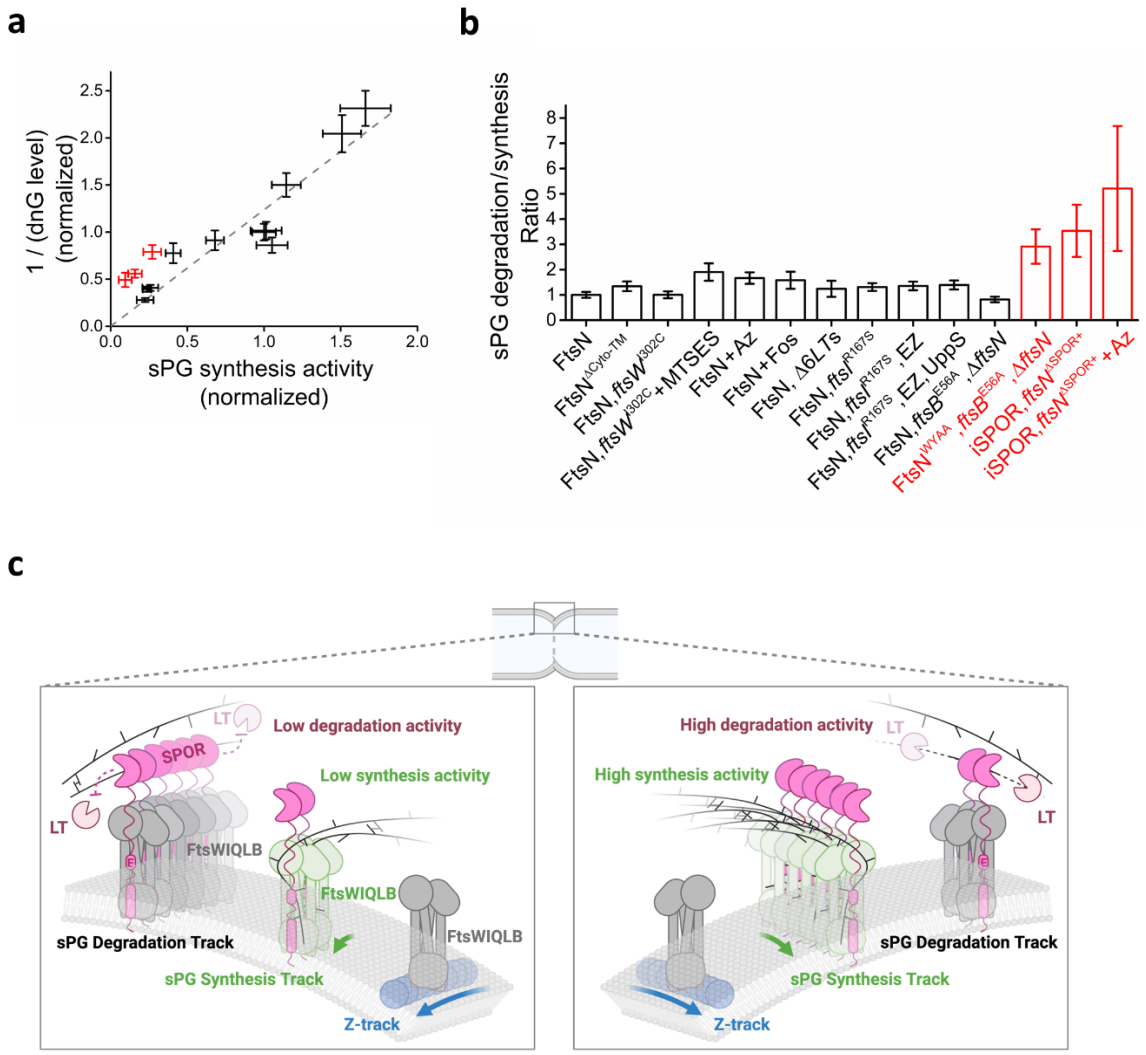

Fig.4 FtsN coordinates sPG synthesis and degradation both in space and time.

a, Apparent sPG synthesis activity, approximated by the product of FtsN's slow-moving population percentage and processive run length, is highly correlated with the apparent sPG degradation activity of LTs, approximated by the inverse of dnG level, across all conditions (black), except when the SPOR domain is unlinked from the rest of the FtsN (red). **b**, The ratio of the apparent sPG degradation to synthesis activity is close to one (black), but became significantly higher when the SPOR domain was unlinked from the rest of the FtsN (red). **c**, A model depicting how FtsN coordinates sPG synthesis and degradation both in space and time. When sPG synthesis activity is low (e.g., under antibiotic treatment), FtsN shifts from the sPG synthesis track to the degradation track. Accumulated SPOR domain binding inhibits LTs' access to degrade dnG, thus decreasing sPG degradation activity. When sPG degradation activity is low, FtsN is constrained either to the Z-track (in the Δ*amiABC* scenario) or the sPG degradation track (in the Δ6*LT*s scenario), thus reducing sPG synthesis activity. Conversely, when sPG synthesis activity is high (e.g., in rich medium), FtsN shifts from the sPG degradation track to the synthesis track, thereby exposing dnG and facilitating its degradation by LTs, consequently increasing sPG degradation activity.